MARKOV CHAIN SIMULATIONS OF VERTICAL DISPERSION FROM ELEVATED SOURCES INTO THE NEUTRAL PLANETARY BOUNDARY LAYER*

P. A. DAVIS

Environmental Research Branch, Whiteshell Nuclear Research Establishment, Pinawa, Manitoba, ROE 1L0, Canada

(Received in final form 2 June, 1983)

Abstract. A Lagrangian statistical-trajectory model based on a Markov chain relation is used to investigate vertical dispersion from elevated sources into the neutral planetary boundary layer. The model is fully two-dimensional, in that both vertical and longitudinal velocity fluctuations, and their correlation, are simulated explicitly. The best observational information currently available is used to characterize the mean and turbulent structure of the neutral boundary layer. In particular, a realistic vertical profile of the Lagrangian integral time scale is proposed, based partly on a review of direct measurements and partly on a comparison of the model predictions with published diffusion data. The model predictions are shown to agree well with a variety of dispersion observations.

The model is used to study vertical diffusion as a function of release height H, friction velocity u_* and surface roughness z_0 for downwind distances up to 10 km from the source. The equivalent Gaussian dispersion parameter σ_z is shown to decrease slightly with an increase in H, and to increase with increases in z_0 or u_*. It is demonstrated that relationships valid in a field of homogeneous turbulence can be applied to vertical dispersion in the atmosphere if the release occurs above the region of strongest gradients in the mean and turbulent parameters. Scaling in terms of the standard deviation in elevation angle of the wind at the release point leads to a universal curve which provides accurate estimates of σ_z over a wide range of values of H, z_0 and the meteorological parameters.

1. Introduction

Lagrangian statistical-trajectory models have recently been used with considerable success to simulate vertical dispersion in the atmosphere. These models predict the concentration field downwind of a given source from the statistics of the trajectories of thousands of fluid elements tracked individually through the atmosphere. Each element is subject to advective transport by a prescribed mean wind field, and to turbulent motion by random velocity fluctuations, which can be generated by a Markov chain relation if the time step of the model is chosen to be much less than the Lagrangian integral time scale, T_L. The advantages of the statistical-trajectory technique over the more traditional approaches to dispersion modelling have been discussed by Wilson *et al.* (1981a) and Sawford (1982), among others.

Smith (1968) was the first to suggest that atmospheric dispersion could be modelled by a Markov chain process. The first calculations were performed by Thompson (1971), who applied the technique to an arbitrary formulation of the problem of diffusion from a stack upwind of a mountain range, and obtained reasonable qualitative results. Hall

* Issued as AECL–7652.

Boundary-Layer Meteorology **26** (1983) 355–376. 0006–8314/83/0264–0355$03.30.

(1975) demonstrated that the technique could in fact produce physically realistic results by simulating observations of dispersion in the atmospheric surface layer under neutral and unstable conditions.

Subsequently, a number of authors have refined the Markov chain model for application to dispersion in the surface layer. Reid (1979) introduced a realistic vertical profile of T_L, and treated elevated as well as surface releases. Wilson *et al.* (1981a) provided insights into the technique through a coordinate transformation, which allowed diffusion in a field of inhomogeneous turbulence to be interpreted in terms of diffusion in a homogeneous field. Vertical variations in the turbulent velocity and length scales were taken into account in an intuitive fashion by Wilson *et al.* (1981b), and more rigorously by Legg and Raupach (1982) in an analysis which demonstrated the connection between the Markov chain procedure and the Langevin equation. Finally, Ley (1982) incorporated detailed information about the structure of the longitudinal component of turbulence into the model, and so was able to model explicitly the vertical momentum flux.

Application of the statistical-trajectory technique to the problem of dispersion throughout the entire depth of the planetary boundary layer (PBL) has been limited by the lack of observations on the vertical variation of the required parameters. Lamb (1978) avoided this difficulty by using wind and turbulence fields generated by Deardorff's boundary-layer turbulence model, to study dispersion from elevated sources in the convective PBL. Reid and Crabbe (1980) and Reid (1981) modelled dispersion in the neutral PBL, but adopted profiles of mean and turbulent wind speeds that were more appropriate to the surface layer. Better profile information is presently becoming available from analyses of the data collected during boundary-layer experiments conducted in Australia (Clarke, 1970; Clarke *et al.*, 1971) and in the United States (Readings *et al.*, 1974). Hanna (1980) has made use of this information in a Markov chain model to determine the effect of release height on dispersion in the unstable PBL over downwind distances on the order of the mixed-layer depth.

It is the purpose of the present paper to use a Markov chain model to investigate vertical dispersion in the neutral PBL for downwind distances up to 10 km from continuous, elevated point sources. The model predictions will be compared with observations, where they exist, and shown to be physically realistic. The effects on dispersion of systematic variations in release height, surface roughness and the meteorological variables will be studied and discussed.

2. Description of the Model

The present model is similar to those described by Reid (1979), Wilson *et al.* (1981a, b) and Legg and Raupach (1982). In each simulation, trajectories of air parcels released from the source are tracked through the atmosphere by integrating the Lagrangian equations:

$$\frac{\mathrm{d}x}{\mathrm{d}t} = u(z, t) = \bar{u}(z) + u'(z, t)\,, \tag{1a}$$

$$\frac{dz}{dt} = w(z,t) = \overline{w}(z) + w'(z,t)\,, \tag{1b}$$

in a coordinate system in which the x-axis is parallel to the mean wind direction and the z-axis is directed vertically upward. $\overline{u}$ and $\overline{w}$ are the mean wind speeds in the x and z directions respectively, and are assumed to be given functions of z. u' and w' are the fluctuating components of the wind and are calculated in a manner to be described below. No motion is allowed in the direction perpendicular to the x-axis in the horizontal plane, so that the results represent either point concentrations due to an infinite line source, or crosswind integrated concentration due to a point source. Trajectories are abandoned once they pass beyond the greatest downwind distance of interest. Trajectories are forced to undergo perfect reflection at $z = z_0$, where z_0 is the surface roughness length; if a trajectory lies below z_0 at the end of a time step, it is relocated an equal distance above z_0 and the sign of its vertical velocity reversed.

Following Smith (1968) and Legg and Raupach (1982), the vertical velocity w at time $t + \Delta t$ is generated from the velocity at some previous time t through a Markov chain expression:

$$w(t + \Delta t) = R_w w(t) + (1 - R_w^2)^{1/2}\, \sigma_w \Gamma + (1 - R_w) T_L\, \partial\sigma_w^2/\partial z \tag{2}$$

where Γ is a random number, chosen by standard numerical techniques, from a Gaussian distribution with zero mean and unit variance. σ_w is the standard deviation in Eulerian vertical velocity, which will be assumed to equal the Lagrangian standard deviation. R_w is the Lagrangian autocorrelation coefficient of vertical velocity at lag time Δt:

$$R_w(\Delta t) = \frac{\overline{w'(t)w'(t + \Delta t)}}{\sigma_w^2}$$

where the overbar denotes an ensemble average. The final term on the right of Equation (2) accounts for the vertical pressure gradient which arises when σ_w is a function of height. Hanna (1979) has shown, through an analysis of tetroon trajectories, that the Markov hypothesis provides an accurate description of turbulent Lagrangian wind speeds in the PBL.

In the limit $\Delta t \to 0$, R_w takes on an exponential form

$$R_w(\Delta t) = \exp(-\Delta t / T_{L_w}) \tag{3}$$

where T_{L_w}, the Lagrangian integral time scale for vertical fluctuations, is given by

$$T_{L_w} = \int_0^\infty R_w(\tau)\, d\tau\,.$$

Expression (3) was used in the present calculations; it is attractive from a theoretical point of view (Tennekes, 1979), and fits the observed data fairly well (Hanna, 1981a).

Time-dependent values of the longitudinal velocity fluctuation u' were generated from a modified Markov relation:

$$s(t + \Delta t) = \alpha s(t) + \gamma\eta$$
$$u'(t + \Delta t) = s(t + \Delta t) + \beta w'(t + \Delta t) . \qquad (4)$$

Here, α, β, and γ are coefficients to be determined, η is a random variate with zero mean and unit variance, and s is a dummy recursive variable. This formulation differs from that of Ley (1982) in that the w' component is not included in the recursive part of Equation (4). This variation was found to be necessary in the present model, in which R_u (the Lagrangian autocorrelation coefficient for u') is assumed to be much larger than R_w near the ground. In such cases, inclusion of the w' term recursively would allow the fluctuating horizontal velocities to build up to large values along those trajectories near the outer edges of the plume, which by their nature are characterized by large vertical velocities of uniform sign over a major part of their history. The result would be artificially large (or small) concentrations, as would become evident if a mass balance were calculated.

Expressions for α, β, and γ can be deduced by applying the following conditions:

(i) The Lagrangian autocorrelation coefficient for u' is given by

$$R_u(\Delta t) = \frac{\overline{u'(t)u'(t + \Delta t)}}{\sigma_u^2}$$

where σ_u is the standard deviation in longitudinal velocity.

(ii) The normalized covariance of the longitudinal and vertical velocity fluctuations takes on a given functional form:

$$\frac{\overline{u'(t)w'(t)}}{\sigma_u\sigma_w} = \frac{-u_*^2}{\sigma_u\sigma_w} = r(z)$$

where u_* is the friction velocity.

(iii) The turbulent energy is conserved:

$$\overline{u'^2}(t) = \sigma_u^2 .$$

Applying these conditions, we obtain:

$$\alpha = (R_u - r^2R_w)/(1 - r^2)$$
$$\beta = r\sigma_u/\sigma_w$$
$$\gamma = \sigma_u[(1 - \alpha^2)(1 - r^2)]^{1/2} .$$

The longitudinal velocity fluctuations have a relatively small effect on the model predictions; for a typical simulation from an elevated source, their inclusion increased $\bar{z}$ and σ_z (integrated statistics of the vertical concentration profiles, defined in Equations (6) and (8) below) by less than 5% at all downwind distances, with the greatest effects occurring within 2 or 3 km of the source.

In routine application of the statistical-trajectory model, the atmosphere was divided into cells of length Δx and height Δz. The length of time spent by each trajectory in each cell was recorded when the trajectory was calculated. If the time spent in cell i by trajectory j is denoted as T_{ij}, then the concentration χ in cell i is given by (Lamb *et al.*, 1979):

$$\chi_i = \left(Q \sum_{j=1}^{N_T} T_{ij} \right) \Big/ (N_T \Delta x \Delta z)$$

where Q is the release rate and N_T the total number of trajectories followed. Confidence in this statistical estimate will be greatest for large values of

$$\sum_{j=1}^{N_T} T_{ij} ,$$

values that can be achieved either by increasing N_T or by expanding the cell dimensions. Neither of these alternatives is particularly attractive, since an increase in N_T results in an increase in computer time, while an increase in Δx or Δz reduces the resolution of the model. In practice, the cells are allowed to expand in size with downwind distance, so that the expected change in concentration across the extent of the cell at a given value of x was limited to a few percent. The number of trajectories required to produce statistically steady results was then determined by examining the trends in intermediate values of χ_i. Typically, between 3000 and 5000 trajectories were necessary to obtain convergence.

The size of the time step used in the integration of Equation (1) determines the scale of dispersion that can be studied by the statistical-trajectory technique. Hall (1975) has shown that it is necessary to have

$$\Delta t \ll T_{L_w} \tag{5}$$

in order to model realistically the dispersion process near the ground. Since T_{L_w} is a function of height in the atmosphere, a convenient way to ensure conformity with Equation (5) at all levels is to set $\Delta t / T_{L_w}$ = constant $\ll 1$. Such a formulation has an additional advantage. We shall see in the next section that, near the ground, $T_{L_w} \sim z/u_*$ and $\partial \bar{u}/\partial z \sim u_*/z$. Thus if Δt is proportional to T_{L_w}, it will also be proportional to $(\partial \bar{u}/\partial z)^{-1}$, the time scale of changes in mean velocity in the vertical, assuring uniform accuracy in the finite-difference solution of Equation (1) at all levels.

A series of simulations carried out using the present model has shown that the predicted values do converge as $\Delta t / T_{L_w}$ is decreased. The calculations discussed below were obtained with $\Delta t / T_{L_w} = 0.1$, a value which produces results within about 4% of those obtained in the limit as $\Delta t / T_{L_w}$ approaches zero, and which is reasonably economical in terms of computer time.

Vertical concentration profiles, calculated using the model described above, were characterized by statistics such as the mass mean height, the profile standard deviation, and the equivalent Gaussian standard deviation, defined respectively by

$$\bar{z}(x) = M_1 / M_0 , \tag{6}$$

$$\sigma_p(x) = [M_2/M_0) - \bar{z}^2]^{1/2}, \tag{7}$$

$$\sigma_z(x) = [M_2/M_0) - H^2]^{1/2} \tag{8}$$

where H is the release height and M_n is the n-th moment of the concentration profile about the surface:

$$M_n(x) = \int_0^\infty \chi(x, z) z^n \, dz . \tag{9}$$

Note that σ_z, as defined in Equation (8), is the standard deviation of mass in a plume that is normally distributed about the level H.

3. The Model Atmosphere

Implementation of the model described above requires detailed knowledge of the mean and turbulent structure of the PBL. This is both a strength and a weakness of the statistical-trajectory technique: it makes maximum use of observational data, but requires information that is not always available. The profiles of $\bar{u}$, u_*, σ_w, σ_u, T_{L_w}, and T_{L_u} (the Lagrangian time scale for longitudinal velocity) used in the present model are based on the best information currently available, and are discussed in turn below.

3.1. $\bar{u}$ Profile

An analytical expression proposed by Long (1974) was adopted for the mean wind profile. Long's expression, which is based on the boundary-layer similarity theory of Csanady (1967) and Gill (1967), takes the form

$$\frac{\bar{u}(z) - U_G}{u_{*0}} = \frac{1}{k}[\ln(\hat{z}/a_1) + a_2(\hat{z}^2 - a_1^2) + a_4(\hat{z}^4 - a_1^4)] \tag{10}$$

where a subscript 0 indicates evaluation of $z = 0$. The parameter k is von Karman's constant, here taken equal to 0.4. The non-dimensional height $\hat{z} = fz/u_{*0}$ has been scaled in terms of the depth h of the neutral PBL:

$$h = a_1 u_{*0}/f$$

where f is the Coriolis parameter. U_G is the longitudinal component of the geostrophic velocity, and is given, together with the transverse component V_G, by the so-called resistance laws:

$$U_G = \frac{u_{*0}}{k}\left[\ln \frac{u_{*0}}{fz_0} - B\right],$$

$$V_G = -Au_{*0}/k . \tag{11}$$

Here A and B are supposedly universal constants under neutral conditions, but published estimates of their values vary widely. We shall adopt $A = 5.0$ and $B = 1.0$, consistent with the recommendations of Arya (1975) and Clarke and Hess (1974).

Specification of Equation (10) is completed by determining the constants a_2 and a_4, which can be found from the boundary conditions (Long, 1974):

$$a_2 = 6(5/4 - B - \ln a_1)/a_1^2\,,$$

$$a_4 = -5\left(a_2/6 + \frac{1}{4a_1^2}\right)\Big/a_1^2\,.$$

Note that Equation (10) reduces to the surface-layer logarithmic profile for small z, and that it is valid only for $z \leq h$.

3.2. u_* Profile

The vertical profile of u_* is also taken from Long (1974), who integrated the equation of motion in the longitudinal direction to obtain

$$\frac{u_*^2(z)}{u_{*0}^2} = 1 - \frac{\hat{z}}{k}\left[b_1\left(\frac{\hat{z}}{2} - a_1\right) + b_2\left(\frac{\hat{z}^3}{4} - a_1^3\right)\right]. \tag{12}$$

The constants b_1 and b_2 were found from application of the boundary conditions to be:

$$b_1 = 3\left(\frac{4k}{3a_1} - A\right)\Big/a_1\,,$$

$$b_2 = \frac{-2}{3a_1^2}\left(b_1 + \frac{2k}{a_1^2}\right).$$

Note that for small z, Equation (12) reduces to

$$u_*(z) = u_{*0}\left(1 - \frac{A}{2k}\,\hat{z}\right) \tag{13}$$

as required near the ground (Panofsky, 1973). The behaviour of u_* at upper levels is also correctly described by Equation (12), which predicts $u_*(h) = 0$.

3.3. σ_w Profile

Surface-layer similarity theory predicts that σ_w at ground level is proportional to u_{*0} in neutral conditions; here we shall assume

$$\sigma_{w0} = 1.3u_{*0}\,, \tag{14}$$

adopting the proportionality constant recommended by Panofsky *et al.* (1977). Measurements by Yokoyama (1971) (reported by Panofsky, 1973), and an analysis by Hojstrup (1982) of the spectra obtained during the Minnesota boundary-layer experiment, suggest that Equation (14) continues to hold up to heights of at least 0.5 h, if the ground-level values σ_{w0} and u_{*0} are replaced by local values:

ground-level values σ_{w0} and u_{*0} are replaced by local values:

$$\sigma_w(z) = 1.3u_*(z)\,. \tag{15}$$

For the present calculations, Equation (15) was assumed to hold throughout the depth of the PBL.

3.4. σ_u Profile

Attempts to apply the simple scaling arguments of the previous section to observations of the longitudinal velocity fluctuations have traditionally been unsuccessful because the low frequency contributions to σ_u are generated by mesoscale terrain features, which are not taken into account in surface-layer similarity theory. However, on the basis of the Minnesota observations, Hojstrup (1982) suggests that, in the neutral limit,

$$\sigma_u = \frac{22u_*}{(1 + 15z/h)^{1/3}}\,.$$

This expression was used in the present calculations.

3.5. T_{L_w} Profile

Physical arguments based on surface-layer similarity theory indicate that, near the ground, T_{L_w} is proportional to z/u_{*0} (Reid, 1979; Hunt and Weber, 1979; Ley, 1982):

$$T_{L_w} = cz/u_{*0}\,. \tag{16}$$

The value of the proportionality constant c is not well known. On the basis of the available observational data, Hunt and Weber (1979) suggest $c = 0.25 \pm 0.12$. A similar value, $c = 0.24$, is obtained by requiring that the length scales for the transport of mass and momentum be equal under neutral conditions. Other investigators using the statistical-trajectory technique have traditionally adopted a c-value that results in the best fit between model predictions and field observations. This approach has yielded values ranging from 0.24 (Ley, 1982) to 0.4 (Reid, 1979; Wilson *et al.*, 1981c).

The behaviour of T_{L_w} above the surface layer was deduced from observations of the vertical velocity spectrum at these heights. The Eulerian time scale T_{E_w} is proportional to $\lambda_{mw}/\bar{u}$ (Pasquill, 1974; Hanna, 1981a), where λ_{mw} is the wavelength at which the logarithmic vertical velocity spectrum attains its maximum value. T_{L_w} is therefore also proportional to $\lambda_{mw}/\bar{u}$ if the hypothesis of Hay and Pasquill (1959) relating Lagrangian and Eulerian time scales is accepted. Observations of λ_{mw} discussed by Hanna (1968), Pasquill (1974), Wamser and Muller (1977) and Grossman (1982) suggest that the linear increase in T_{L_w} with z is not maintained above the surface layer; rather, T_{L_w} must increase more slowly here, and eventually become uniform or decrease with height.

Observations of the magnitude of T_{L_w} above the surface layer have been collected in Table I. The values presented by Draxler (1976) and Neumann (1978) may not be very reliable since they were deduced by fitting a function of T_{L_w} to measured dispersion data that showed considerable scatter. In addition, although the sources in these experiments were for the most part elevated, the dispersion measurements themselves were made at ground level, so that it is not clear at what height these T_{L_w} values should be applied. The values quoted by Hanna (1979, 1981a) were derived from the Lagrangian autocorrelograms formed from direct measurements of the position of neutrally buoyant balloons. The direct measurements might overestimate the neutral value of T_{L_w} to some degree, since they were obtained under unstable conditions. The values shown in Table I are reasonably consistent with the hypothesis that $T_{L_w} \sim 100$ s, independent of height above 300 m in neutral conditions.

TABLE I

Observations and estimates of T_{L_w} above the surface layer

Observer	Height of measurement (m)	Stability	T_{L_w} (s)
Draxler (1976)	elevates sources (46–152 m)	stable	60
		unstable	300
Neumann (1978)	surface and elevated sources (108 m)	neutral	70
Hanna (1979)			
Las Vegas data	400–500	daytime conditions	57
Idaho Falls data	mid PBL	unstable	163
Hanna (1981a)	300	unstable	70
	700	unstable	90

Hanna (1981b) has recently suggested that the functional dependence of T_{L_w} upon height can be described analytically by

$$T_{L_w} = \frac{cz}{u_{*0}} \frac{1}{1 + \mathrm{d}\hat{z}}, \tag{17}$$

where d is a constant. Profile (17) increases monotonically with height, asymptotically approaching a value of $c/(\mathrm{d}f)$ at great heights. This asymptotic value is independent of u_{*0}, in agreement with observations by Hanna (1968). A value $d = 40$ ensures that $T_{L_w} \sim 100$ s at great heights if $c = 0.4$. Although the observational evidence for these values is not conclusive, it will be shown in Section 4 that they produce results in good agreement with diffusion measurements.

3.6. T_{L_u} Profile

In the absence of direct measurements, information on the T_{L_u} profile must come from the available observations of the vertical variation of the longitudinal velocity spectrum. The data summary presented by Pasquill (1974), and the analyses of the Minnesota observations by Kaimal *et al.* (1976) and Hojstrup (1982), indicate that the shape and scale of the u-spectrum change only slowly with height in the neutral PBL. The ratio $\lambda_{mu}/\lambda_{mw}$, where λ_{mu} is the peak wavelength in the u-spectrum, is approximately 10 near the ground and unity at upper levels, where the spectra of all three velocity components take on the same shape. Accordingly, we adopt a profile

$$T_{L_u} = \frac{c}{fd}\,(1 - e^{-400\hat{z}})\,,$$

which ensures that T_{L_u} shows little height dependence throughout most of the PBL, with $T_{L_u} \sim 10\,T_{L_w}$ near the ground and $T_{L_u} = T_{L_w}$ at great heights.

4. Comparison of Model Predictions with Observations

There exist very few direct observations of vertical dispersion against which to compare the model predictions. Dispersion in the surface layer was well-documented in the Project Prairie Grass (PPG) experiments (Barad, 1958; Haugen, 1959), and these results will be used to verify the predictions of the model near the ground. At greater heights, the model results will be compared with the observations from an elevated source obtained by Högstrom (1964) in Sweden.

The PPG experiments were carried out in Nebraska at latitude 42° N over flat, uniform terrain characterized by $z_0 = 0.8$ cm. Vertical concentration profiles were measured 100 m downwind from a continuous point source of sulphur dioxide, located at a height of 0.46 m. The profiles obtained under neutral conditions were characterized by $\bar{z} = 3.5$ m (Nieuwstadt and van Ulden, 1978) and $\sigma_m = 4.5$ m (Pasquill, 1974), where

$$\sigma_m^2 = \sigma_z^2 + H^2\,.$$

Data listed by van Ulden (1978) indicate a mean value $u_{*0} = 0.41$ m s^{-1} for the near-neutral runs (runs for which $|L| > 150$ m, where L is the Monin-Obukhov length).

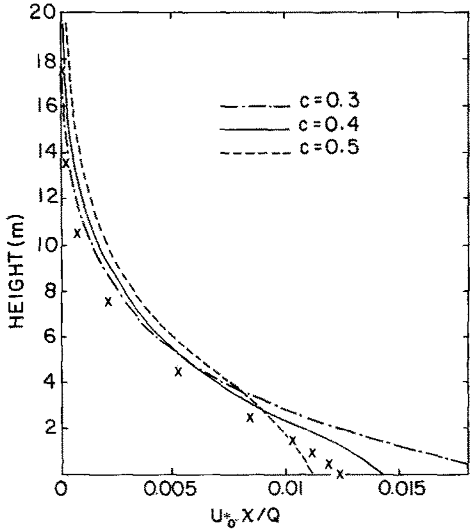

Fig. 1. Observed (discrete points) and predicted (continuous curves) vertical concentration distribution under neutral conditions at Project Prairie Grass for three values of the parameter c. $d = 40$.

The mean cross-wind integrated concentration profile observed at PPG under neutral conditions is compared with the model predictions in Figure 1 for three values of the parameter *c*. In these calculations, *d* was set equal to 40, although the results are not sensitive to the precise value of this parameter. The value $c = 0.4$ provides a good overall fit to the observed profile, as concluded previously by Wilson *et al.* (1981c), and allows for a slight loss of SO_2 at the surface through dry deposition.

With $c = 0.4$, the predicted values of $\bar{z}$ and σ_m are 4.15 and 5.50 m, respectively, some 20% higher than the observations. This discrepancy cannot be considered significant, however, since variations of this size can result from only minor changes in profile shape. In addition, the observed profiles were defined by relatively few observations at upper levels, which are the levels to which determinations of $\bar{z}$ and σ_m are most sensitive.

Högstrom's (1964) study was carried out at a latitude of 59° N at Agesta, Sweden, over rolling forested terrain characterized by $z_0 = 0.59$ m. A series of 30-s smoke puffs, released sequentially from a height of 50 m, was photographed to yield estimates of the standard deviation of material within each puff, and the standard deviation of the displacement about the puff centres. These two measurements were then combined to give the total spread of material. Although these results are based on a quasi-instantaneous source, the analysis of Hunt and Weber (1979) indicates that they may be applied with little error to a continuous source.

The comparison of Högstrom's neutral observations with model predictions is shown in terms of σ_z in Figure 2, with $c = 0.4$, $u_{*0} = 0.51$ m s^{-1} (as indicated by wind profile measurements at the site), and three different values of *d*. Good agreement is obtained with $d = 40$, a value consistent with the observations of T_{L_w} discussed in the previous section.

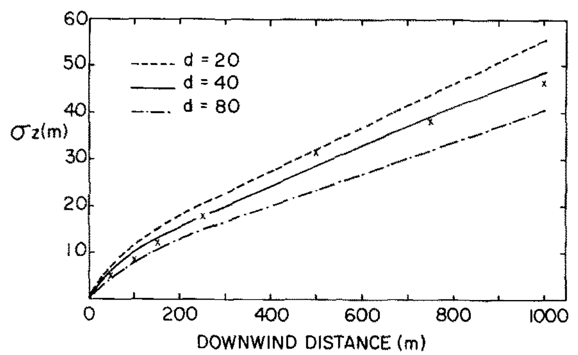

Fig. 2. Observed (discrete points) and predicted (continuous curves) variation of σ_z with downwind distance under neutral conditions at Agesta, Sweden, for three values of the parameter *d*. $c = 0.4$.

The statistical-trajectory model therefore appears able to simulate realistically vertical dispersion in the lower level of the neutral PBL. In the following section, the model will be extended to determine the characteristics of dispersion throughout the PBL as a function of z_0, H, and u_{*0}, for downwind distances up to 10 km from the source.

5. PBL Simulations

In each PBL simulation, $\Delta t/T_{L_w}$ and a_1 were assigned values of 0.1 and 0.2, respectively. A run out to 10 km typically required about 15 min of CPU time on a CDC 6600 computer.

The numerical predictions for σ_z will first be compared with three standard curves that are commonly used to estimate σ_z. These curves were not used in the previous section to calibrate the T_{L_w} profile, or to verify the model predictions, since they were deduced indirectly from ground-level concentrations measurements and the principle of conservation of mass. The values of H, z_0, u_{*0}, and f used in the simulations were chosen to agree with the values observed at the sites where the standard curves were developed.

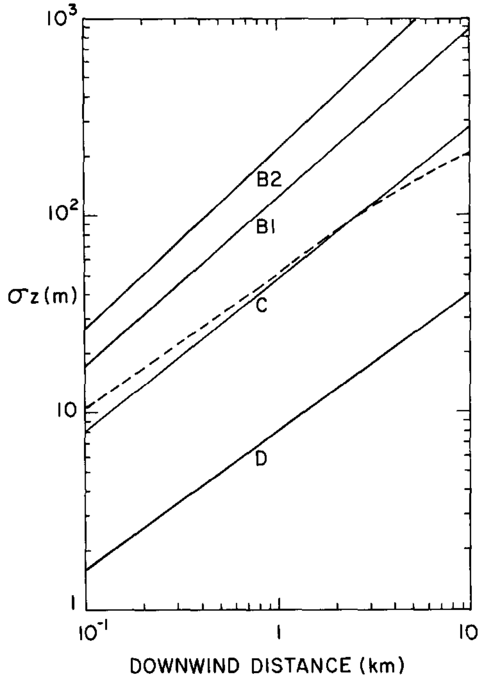

Fig. 3. Comparison of Brookhaven σ_z curves (solid lines) with the model predictions (dashed line) for neutral conditions, with $H = 100$ m, $z_0 = 1$ m, $f = 9.5 \times 10^{-5}$ s^{-1} and $u_{*0} = 0.63$ m s^{-1}. The letters denote Brookhaven stability class.

Figure 3 shows the comparison with the Brookhaven curves (Singer and Smith, 1966), assuming $H = 100$ m, $z_0 = 1$ m, $u_{*0} = 0.63$ m s^{-1}, and $f = 9.5 \times 10^{-5}$ s^{-1}. The agreement with the neutral (class C) curve is as good as can be expected given that the Brookhaven results are expressed as power laws. The comparison with Briggs' (1974) curves is shown in Figure 4. Although Briggs' curves are based for the most part on diffusion experiments from ground-level sources, a value $H = 25$ m was adopted here (together with $z_0 = 0.03$ m, $u_{*0} = 0.45$ m s^{-1} and $f = 1.15 \times 10^{-4}$); smaller values of

H require considerably greater amounts of computer time. Despite this difference, the calculated σ_z curve agrees quite well with Briggs' neutral (Pasquill class D) curve, apart from an over-estimation of about 20% close to the source. This discrepancy is similar in magnitude to that found between observed and predicted σ_z values in the PPG simulation.

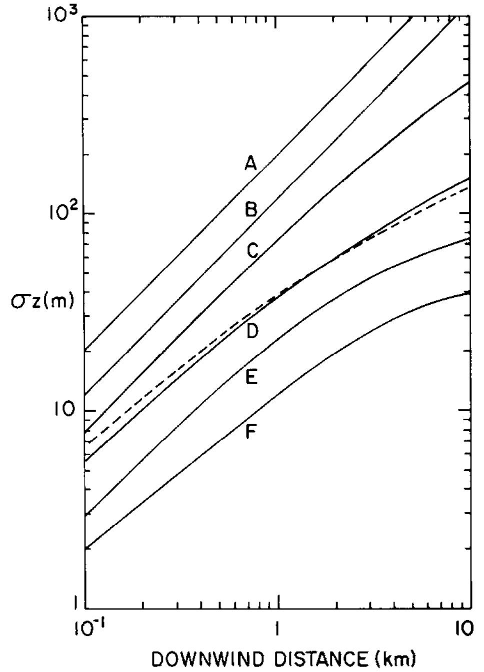

Fig. 4. Comparison of Briggs' σ_z curves (solid lines) with the model predictions (dashed line) for neutral conditions, with $H = 25$ m, $z_0 = 0.03$ m, $f = 1.15 \times 10^{-4}$ s^{-1}, and $u_{*0} = 0.45$ m s^{-1}. The letters denote Pasquill stability class.

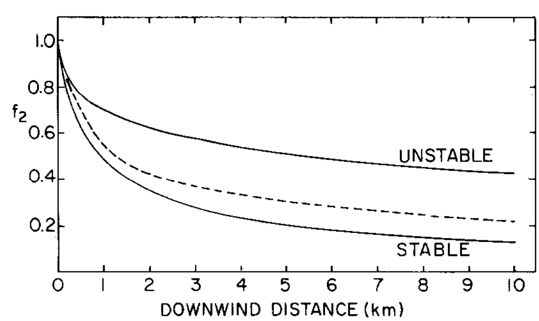

Fig. 5. Comparison of Draxler's function f_2 (solid lines) with the model predictions (dashed line), with $H = 100$ m, $z_0 = 0.1$ m, $f = 1.11 \times 10^{-4}$ s^{-1}, and $u_{*0} = 0.5$ m s^{-1}. In the numerical analysis, σ_ϕ was evaluated at $z = H$.

The final comparison is with the formulation for σ_z developed by Draxler (1976), who assumed that

$$\sigma_z/(\sigma_\phi x) = f_2(T/T_{L_w}) \tag{18}$$

where f_2 is a universal function and T is the travel time of an air parcel from the source to downwind distance x. Figure 5 shows the comparison betwen Draxler's expressions for f_2 for elevated releases and the left-hand side of Equation (18), evaluated from the numerical calculations at the release height assuming $z_0 = 0.1$ m, $H = 100$ m, $u_{*0} = 0.5$ m s^{-1}, and $f = 1.11 \times 10^{-4}$ s^{-1}. The results are presented in terms of downwind distance rather than travel time, where it has been assumed that the two variables are related through the mean wind speed at the release height (8.72 m s^{-1} for this simulation). The numerical curve strikes a reasonable balance between Draxler's stable and unstable results.

The good agreement between the model predictions for σ_z and the standard curves indicates that the trajectory model provides a realistic simulation of dispersion in the neutral PBL over a wide range of release heights and surface roughnesses. The predictions of the model under systematic variations in H, u_{*0}, and z_0 will now be examined.

The dependence of the dispersion process on release height is shown in Figure 6, in which $\bar{z}$, σ_z, and χ_0/Q (the normalized ground-level concentration) are shown as functions of downwind distance for four different values of H, with z_0, and u_{*0} fixed at 0.1 m and 0.5 m s^{-1}, respectively. The effects of release height on $\bar{z}$ and χ_0/Q are pronounced near the source, but diminish farther downwind as the plume is mixed through a deeper layer. The dispersion parameter σ_z decreases slightly with H at all

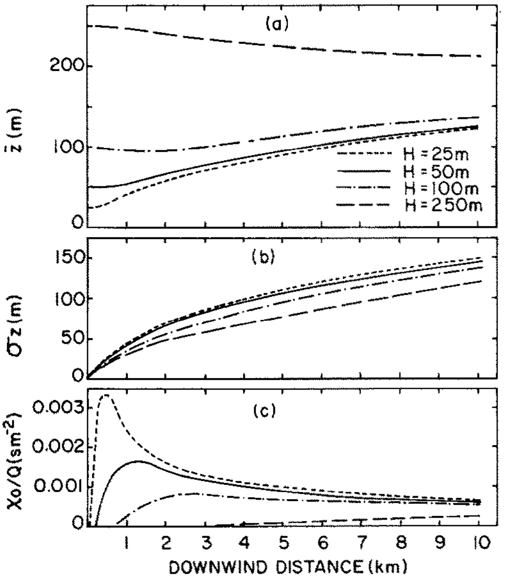

Fig. 6. Variation with downwind distance and release height of (a) $\bar{z}$; (b) σ_z; and (c) normalized ground-level concentration. $z_0 = 0.1$ m, $f = 1.11 \times 10^{-4}$ s^{-1} and $u_{*0} = 0.5$ m s^{-1}.

downwind distances. This result is to be expected with the present model, in which σ_ϕ decreases away from the ground, and is in agreement with the qualitative discussion given by Hanna (1980). However, the reverse effect is apparent in two experimental studies that have addressed this question. Vogt *et al.* (1978) report that measurements taken within 10 km of the source under neutral conditions indicated a slight increase in σ_z as H was increased from 50 to 100 m. The σ_z values used in their study were deduced from ground-level concentration measurements, however, so that the small differences between these findings and the present results are probably not significant. Doran *et al.* (1978) also report an increase in σ_z with H, in this case a 50% increase at a downwind distance of 400 m as H was increased from 26 to 56 m. However, the σ_z values used in that study were again deduced indirectly, and in addition were obtained under stable conditions; they may not be relevant to the present discussion, therefore.

The effect of friction velocity on $\bar{z}$, σ_z, and χ_0/Q is shown in Figure 7, in which H and z_0 have been set equal to 50 and 0.1 m, respectively. In the present model, the ratio $\sigma_w/\bar{u}$, and therefore the rate of growth of the plume, increase with u_{*0}. In contrast, an increase in u_{*0} leads to a decrease in T_{L_w} and a consequent reduction in the plume spread. The net effect of these two processes is an increase in $\bar{z}$ and σ_z with u_{*0}, as shown in Figure 7,

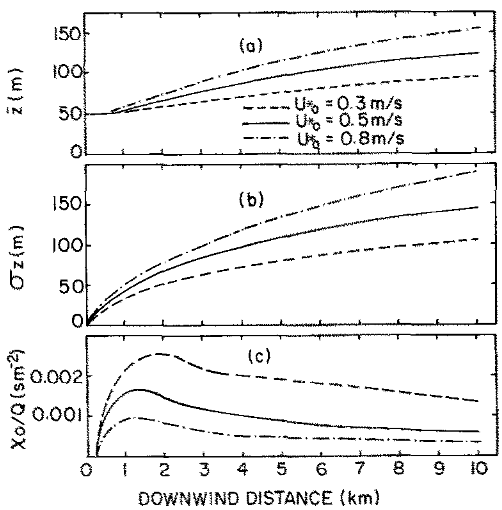

Fig. 7. Variation with downwind distance and friction velocity of (a) $\bar{z}$; (b) σ_z; and (c) normalized ground-level concentration. $z_0 = 0.1$ m, $H = 50$ m, and $f = 1.11 \times 10^{-4}\ \mathrm{s}^{-1}$.

together with a shift in the location of the maximum ground-level concentration to smaller downwind distances. Smaller values of u_{*0} lead to lower wind speeds throughout the PBL, and so to smaller volumes of air in which a contaminant can be diluted. The result is a decrease in χ_0/Q with increased u_{*0}, as shown in Figure 7(c).

The dependence of $\bar{z}$, σ_z, and χ_0/Q upon surface roughness is examined in Figure 8, in which H has been set to 50 m. In these simulations, the geostophic velocity U_G was held constant at $12\ \mathrm{m\,s^{-1}}$, and a separate value of u_{*0} was calculated from

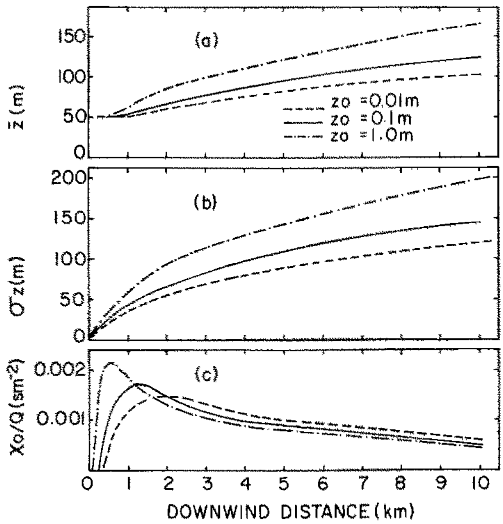

Fig. 8. Variation with downwind distance and surface roughness of (a) $\bar{z}$; (b) σ_z; and (c) normalized ground-level concentration. $H = 50$ m, $f = 1.11 \times 10^{-4}$ s^{-1} and $u_{*0} = 0.41$, 0.50, and 0.63 m s^{-1}, respectively, for the simulations with $z_0 = 0.01$, 0.1, and 1 m.

Equation (11) for each value of z_0. In this way, the results can be interpreted in terms of dispersion in a given large-scale flow which passes over terrain of varying surface roughness, and which comes into equilibrium with each surface in turn. With this convention, an increase in z_0 leads to an increase in the ratio $\sigma_w/\bar{u}$, and enhanced dispersion at all downwind distances, accompanied by a shift in the location of the maximum ground-level concentration to smaller distances. The increase in the maximum of χ_0/Q with z_0 arises from the fact that, in the model, larger values of z_0 are associated with smaller wind speeds throughout the lower levels of the PBL.

The dependence of σ_z upon z_0 is frequently expressed through the relation $\sigma_z \sim z_0^p$, so that p can be evaluated from

$$p = \ln(\sigma_{za}/\sigma_{zb})/\ln(z_{0a}/z_{0b})$$

if values of σ_z appropriate to the two roughness lengths z_{0a} and z_{0b} are known. Values

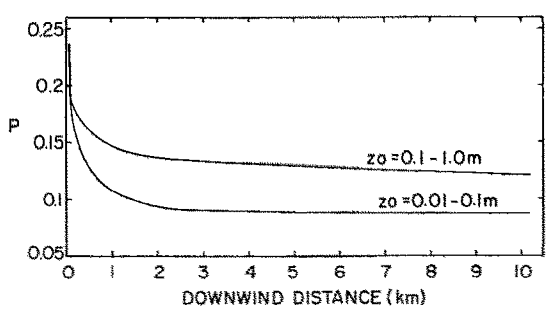

Fig. 9. Variation with downwind distance and surface roughness of the exponent p in $\sigma_z \sim z_0^p$.

of p are shown in Figure 9, in which the lower and upper curves were determined using paired z_0 values of 0.01 and 0.1 m, and 0.1 and 1 m, respectively. Very close to the source, p takes on relatively large values independent of z_0. At larger downwind distances, p decreases at a rate which is dependent upon z_0; the larger values of p are associated with the rougher surfaces. These findings are in agreement with the experimental values of p discussed by Pasquill (1975).

The numerical values of σ_z are compared in Figure 10 with the curves of Smith (1972) and Hosker (1974), which are explicit functions of z_0. Although there is general agreement between the two sets of curves, there are significant differences also. They each show essentially the same dependence on z_0 at small and intermediate values of z_0, while the present results show a stronger dependence of σ_z on z_0 over rough surfaces. For $z_0 \leq 0.1$, the present values of σ_z exceed the Smith-Hosker values at small downwind distances, while the reverse is true at greater distances. For $z_0 = 1$ m, the present values of σ_z are larger than the Smith-Hosker values at all distances, although the shape of the two curves is similar. It is not unreasonable that the two sets of curves differ in magnitude near the source, since the Smith-Hosker curves apply to releases near the ground, while a value $H = 50$ m was adopted for the numerical calculations. However, the sense of the difference in magnitude is opposite to what might have been expected, and the difference does not become small at larger downwind distances, as it would if it were due entirely to an inappropriate choice for H.

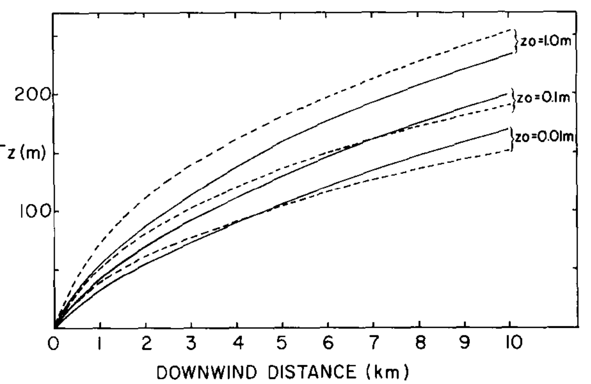

Fig. 10. Comparison of the Smith-Hosker σ_z curves (solid lines) with the model predictions (dashed lines) for three values of z_0. $H = 50$ m, $f = 1.11 \times 10^{-4}$ s^{-1}, $U_G = 20$ m s^{-1}, and $u_{*0} = 0.65, 0.80$, and 0.99 m s^{-1}, respectively, for simulations with $z_0 - 0.01$, 0.1, and 1 m.

It should be noted that the results shown in Figure 10 were obtained with $U_G = 20$ m s^{-1}. The smaller values of U_G used in the simulations previously discussed lead to much poorer agreement between the 2 sets of curves. The Smith-Hosker curves therefore appear to give the best results when applied under conditions of strong winds.

An attempt was made to organize the predicted values of σ_z in terms of Draxler's (1976) theory as represented by Equation (18). The parameter values used in the simulations that were run for this analysis are given in Table II. Application of

TABLE II

Parameter values for the simulations presented in Figures 11 and 12

Simulation	z_0 (m)	U_G (m s^{-1})	u_{*0} (m s^{-1})	H (m)	f (s^{-1})
0	0.01	12.0	0.41	50	1.11×10^{-4}
1	0.1	12.0	0.5	25	1.11×10^{-4}
2	0.1	6.9	0.3	50	1.11×10^{-4}
3	0.1	12.0	0.5	50	1.11×10^{-4}
4	0.1	12.5	0.5	50	7.27×10^{-5}
5	0.1	11.7	0.5	50	1.41×10^{-4}
6	0.1	20.0	0.8	50	1.11×10^{-4}
7	0.1	12.0	0.5	100	1.11×10^{-4}
8	0.1	12.0	0.5	250	1.11×10^{-4}
9	1.0	12.0	0.63	50	1.11×10^{-4}

Equation (18) in a field of vertically inhomogeneous turbulence is made difficult by the need to characterize the spread of the plume in terms of turbulence measurements made at a single height. There are two obvious choices for this height, H and $\bar{z}$, with $\bar{z}$ perhaps being the more natural since this is the level at which the bulk of the plume resides. A plot of $\sigma_z/(x\sigma_\phi)$ versus T/T_{L_w}, in which σ_ϕ, $\bar{u}$ and T_{L_w} have been evaluated at $\bar{z}$, is shown in Figure 11. This scaling is quite effective in organizing the data, especially at the larger downwind distances where $\bar{z}$ becomes essentially independent of H. Although it does not appear possible to produce an entirely universal curve through scaling according to

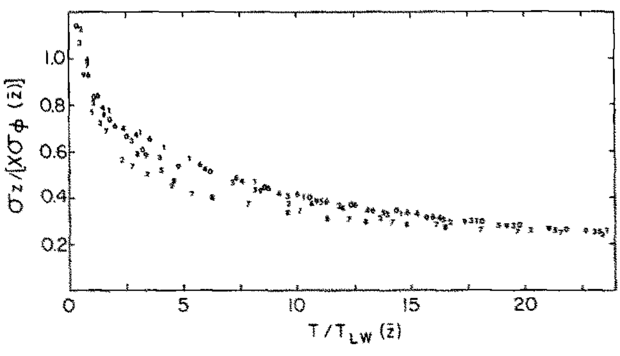

Fig. 11. Variation of $\sigma_z/(x\sigma_\phi)$ with T/T_{L_w}. σ_ϕ, $\bar{u}$, and T_{L_w} have been evaluated at $z = \bar{z}$. The curves are depicted by numbers which correspond to the simulations listed in Table II.

Equation (18), the scatter evident in Figure 11 is impressively small considering the wide range of parameter values which the data represent. The small scatter also suggests that relationships, such as Equation (18), which assume the existence of a homogeneous turbulence field, can be applied to vertical dispersion in the atmosphere if the release occurs above the region of strongest gradients in the mean and turbulent parameters.

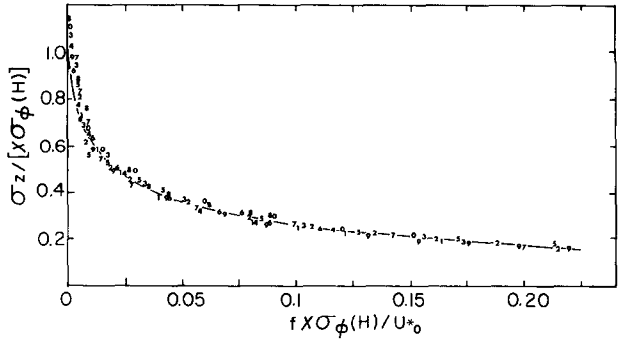

Fig. 12. Variation of $\sigma_z/(x\sigma_\phi)$ with $\hat{x}\sigma_\phi$. σ_ϕ has been evaluated at $z = H$. The curves are depicted by numbers which correspond to the simulations listed in Table II. The solid line corresponds to Equation (19).

It is unlikely that estimates of $\bar{z}$ or T_{L_w} will be available in most practical situations where a value of σ_z is required. A simpler form of Equation (18),

$$\sigma_z/(x\sigma_\phi) = f_3(x)$$

was investigated in analogy with an expression suggested by Pasquill (1976) for the horizontal dispersion parameter σ_y, but this scaling leads to scatter that is too great to make the results particularly useful. On the other hand, Figure 12 shows that the predictions collapse into a universal curve when the data are scaled according to

$$\sigma_z/(x\sigma_\phi) = f_4(\hat{x}\sigma_\phi)$$

where $\hat{x} = fx/u_{*0}$ and σ_ϕ is evaluated at $z = H$. The curve drawn through the data points has the form

$$\frac{\sigma_z}{x\sigma_\phi} = \frac{1}{1 + 14.7(\hat{x}\sigma_\phi)^{0.69}} \tag{19}$$

Equation (19) provides a simple means for the reliable prediction of σ_z over a wide range of values of H, z_0 and the meteorological parameters. Estimates of $\sigma_\phi(H)$ and u_{*0} can be obtained fairly easily by direct measurements, or indirectly from routine meteorological observations (Draxler, 1979).

6. Conclusions

The results of the previous section indicate that the statistical-trajectory model can simulate realistically vertical dispersion in the neutral PBL within 10 km of elevated point sources. This in turn implies that the profiles adopted here for σ_w and T_{L_w} are also realistic, to a height of at least 500 m. The statistical-trajectory model is therefore available, as an alternative to the more traditional dispersion models, to investigate complex problems of atmospheric diffusion in the PBL.

The main conclusions to emerge from the present study are summarized below:

(i) At all downwind distances, σ_z decreases slightly with an increase in release height.

(ii) Larger values of u_{*0} result in larger values of $\bar{z}$ and σ_z, and a reduction in ground-level concentrations.

(iii) An increase in z_0 leads to enhanced dispersion at all downwind distances. Over rough surfaces, the present model predicts a stronger dependence of σ_z on z_0 than do the σ_z curves of Smith (1972) and Hosker (1974). The latter curves appear to apply best to strong-wind conditions.

(iv) Relationships valid in a field of homogeneous turbulence can be applied to vertical dispersion in the atmosphere if the release occurs above the region of strongest gradients in the mean and turbulent parameters. In a vertically inhomogeneous atmosphere, the spread of a plume can be characterized reasonably well by local statistics of turbulence if the statistics are measured at a height $\bar{z}(x)$.

(v) Scaling in terms of f/u_{*0}, a measure of the depth of the neutral PBL, and in terms of $\sigma_\phi(H)$, the standard deviation in elevation angle measured at the release height, leads to a universal curve (Equation (19)) which provides accurate estimates of σ_z over a wide range of values of H, z_0 and the meteorological parameters.

References

Arya, S. P. S.: 1975, 'Geostrophic Drag and Heat Transfer Relations for the Atmospheric Boundary Layer', *Quart. J. Roy. Meteorol. Soc.* **101**, 147–161.

Barad, M. L.: 1958, 'Project Prairie Grass, a Field Program in Diffusion (Vol. II)', Geophysical Research Paper No. 59, Air Force Cambridge Research Centre-TR-58-235 (II).

Briggs, G. A.: 1974, 'Diffusion Estimation for Small Emissions', in Environment Research Laboratories, Air Resources Atmospheric Turbulence and Diffusion Laboratory, 1973 Annual Report, USAEC Report ATDL-106, National Oceanic and Atmospheric Administration, December 1974.

Clarke, R. H.: 1970, 'Observational Studies in the Atmospheric Boundary Layer', *Quart. J. Roy. Meteorol. Soc.* **96**, 91–114.

Clarke, R. H. and Hess, G. D.: 1974, 'Geostrophic Departure and the Functions A and B of Rossby-Number Similarity Theory', *Boundary-Layer Meteorol.* **7**, 267–287.

Clarke, R. H., Dyer, A. J., Brook, R. R., Reid, D. G., and Troup, A. J.: 1971, 'The Wangara Experiment: Boundary Layer Data', Tech. Paper No. 19, CSIRO, Div. Meteor. Phys. Aspendale, Australia, 362 pp.

Csanady, G. T.: 1967, 'On the Resistance Law of a Turbulent Ekman Layer', *J. Atmos. Sci.* **24**, 467–471.

Deardorff, J. W.: 1974, 'Three-Dimensional Study of the Height and Mean Structure of a Heated Planetary Boundary Layer', *Boundary-Layer Meteorol.* **7**, 81–106.

Doran, J. C., Horst, T. W., and Nickola, P. W.: 1978, 'Experimental Observations of the Dependence of Lateral and Vertical Dispersion Characteristics on Source Height', *Atmos. Environ.* **12**, 2259–2263.

Draxler, R. R.: 1976, 'Determination of Atmospheric Diffusion Parameters', *Atmos. Environ.* **10**, 99–105.

Draxler, R. R.: 1979, 'Estimating Vertical Diffusion from Routine Meteorological Tower Measurements', *Atmos. Environ.* **13**, 1559–1564.

Gill, M. E.: 1967, 'The Turbulent Ekman Layer', Dept. Applied Mathematics and Theoretical Physics, University of Cambridge, England (unpublished manuscript).

Grossman, R. L.: 1982, 'An Analysis of Vertical Velocity Spectra Obtained in the BOMEX Fair-Weather, Trade-Wind Boundary Layer', *Boundary-Layer Meteorol.* **23**, 323–357.

Hall, C. D.: 1975, 'The Simulation of Particle Motion in the Atmosphere by a Numerical Random-Walk Model', *Quart. J. Roy. Meteorol. Soc.* **101**, 235–244.

Hanna, S. R.: 1968, 'A Method of Estimating Vertical Eddy Transport in the Planetary Boundary Layer using Characteristics of the Vertical Velocity Spectrum', *J. Atmos. Sci.* **25**, 1026–1033.

Hanna, S. R.: 1979, 'Some Statistics of Lagrangian and Eulerian Wind Fluctuations', *J. Appl. Meteorol.* **18**, 518–525.

Hanna, S. R.: 1980, 'Effects of Release Height on σ_y and σ_z in Daytime Conditions', in Plume Diffusion Modelling, Annual Report to the Nuclear Regulatory Commission, Air Resources Atmospheric Turbulence and Diffusion Laboratory, ATDL-80/24, September, 1980.

Hanna, S. R.: 1981a, 'Lagrangian and Eulerian Time Scale Relations in the Daytime Boundary Layer', *J. Appl. Meteorol.* **20**, 242–249.

Hanna, S. R.: 1981b, 'Turbulent Energy and Lagrangian Time Scales in the Planetary Boundary Layer', Preprints of the Fifth Symposium on Turbulence, Diffusion and Air Pollution, Atlanta, March 1981, American Meteorological Society, Boston.

Haugen, D. A.: 1959, 'Project Prairie Grass, a Field Program in Diffusion (Vol. III)', Geophysical Research Papers No. 59, Air Force Cambridge Research Centre-TR-58-235 (III).

Hay, J. S. and Pasquill, F.: 1959, 'Diffusion from a Continuous Source in Relation to the Spectrum and Scale of Turbulence', *Adv. Geophys.* **6**, 345.

Högstrom, U.: 1964, 'An Experimental Study on Atmospheric Diffusion', *Tellus*, 205–251.

Hojstrup, J.: 1982, 'Velocity Spectra in the Unstable Planetary Boundary Layer', *J. Atmos. Sci.* **39**, 2239–2248.

Hosker, R. P., Jr.: 1974, 'Estimates of Dry Deposition and Plume Depletion over Forests and Grassland', in Physical Behaviour of Radioactive Contaminants in the Atmosphere, IAEA, STI/PB/354,291–309.

Hunt, J. C. R. and Weber, A. H.: 1979, 'A Lagrangian Statistical Analysis of Diffusion from a Ground-Level Source in a Turbulent Boundary Layer', *Quart. J. Roy. Meteorol. Soc.* **105**, 423–443.

Kaimal, J. C., Haugen, D. A., Coté, O. R., Izumi, Y., Caughey, S. J., and Readings, C. J.: 1976, 'Turbulence Structure in the Convective Boundary Layer', *J. Atmos. Sci.* **33**, 2152–2169.

Lamb, R. G.: 1978, 'A Numerical Simulation of Dispersion from an Elevated Point Source in the Convective Planetary Boundary Layer', *Atmos. Environ.* **12**, 1297–1304.

Lamb, R. G., Hogo, H., and Reid, L. E.: 1979, 'A Lagrangian – Monte Carlo Model of Air Pollution Transport, Diffusion and Removal Processes', Preprints of the Fourth Symposium on Turbulence, Diffusion and Air Pollution, American Meteorological Society, Boston.

Legg, B. J. and Raupach, M. R.: 1982, 'Markov-Chain Simulation of Particle Dispersion in Inhomogeneous Flows: The Mean Drift Velocity Induced by a Grandient in Eulerian Velocity Variance', *Boundary-Layer Meteorol.* **24**, 3–13.

Ley, A. J.: 1982, 'A Random Walk Simulation of Two-Dimensional Turbulent Diffusion in the Neutral Surface Layer', *Atm. Environ.* **16**, 2799–2808.

Long, R. R.: 1974, 'Mean Stresses and Velocities in the Neutral, Barotropic Planetary Boundary Layer', *Boundary-Layer Meteorol.* **7**, 475–487.

Neumann, J.: 1978, 'Some Observations on the Simple Exponential Function as a Lagrangian Velocity Correlation Function in Turbulent Diffusion', *Atmos. Environ.* **12**, 1965–1968.

Nieuwstadt, F. T. M. and Van Ulden, A. P.: 1978, 'A Numerical Study on the Vertical Dispersion of Passive Contaminants from a Continuous Source in the Atmospheric Surface Layer', *Atmos. Environ.* **12**, 2119–2124.

Panofsky, H. A.: 1973, 'Tower Micrometeorology', in D. A. Haugen (ed.), Workshop on Micrmeteorology, American Meteorological Society, Boston.

Panofsky, H. A., Tennekes, H., Lenschow, D. H., and Wyngaard, J. C.: 1977, 'The Characteristics of Turbulent Velocity Components in the Surface Layer under Convective Conditions', *Boundary-Layer Meteorol.* **11**, 355–361.

Pasquill, F.: 1974, '*Atmospheric Diffusion*', John Wiley and Sons, New York, N.Y., 429 pp.

Pasquill, F.: 1975, 'The Dispersion of Materials in the Atmospheric Boundary-Layer – The Basis for Generalization', Lectures on Air Pollution and Environmental Impact Analyses, American Meteorological Society, Boston, 1–34.

Pasquill, F.: 1976, 'Atmospheric Dispersion Parameters in Gaussian Plume Modelling, Part 2, Possible Requirements for Change in the Turner Workbook Values', EPA-600/4-76-030b, Washington, D.C.

Readings, C. J., Haugen, D. A., and Kaimal, J. C.: 1974, 'The 1973 Minnesota Atmospheric Boundary Layer Experiment', *Weather* **29**, 309–312.

Reid, J. D.: 1979, 'Markov Chain Simulations of Vertical Dispersion in the Neutral Layer for Surface and Elevated Releases', *Boundary-Layer Meteorol.* **16**, 3–22.

Reid, J. D.: 1981, 'The Appropriate Choice of σ_z and $\bar{u}$ for Predicting Surface Concentration using the

Gaussian Model', Proceedings, Air Pollution Sessions, Fifteenth Annual Congress of the Canadian Meteorological and Oceanographic Society, Saskatoon, May, 1981.

Reid, J. D. and Crabbe, R. S.: 1980, 'Two Models of Long-Range Drift of Forest Pesticide Aerial Spray', *Atmos. Environ.* **14**, 1017–1025.

Sawford, B. L.: 1982, 'Lagrangian Monte Carlo Simulation of the Turbulent Motion of a Pair of Particles', *Quart. J. Roy. Meteorol. Soc.* **108**, 207–213.

Singer, I. A. and Smith, M. E.: 1966, 'Atmospheric Dispersion at Brookhaven National Laboratory', *Int. J. Air Water Pollut.* **10**, 125–135.

Smith, F. B.: 1968, 'Conditioned Particle Motion in a Homogeneous Turbulent Field', *Atmos. Environ.* **2**, 491–508.

Smith, F. B.: 1972, 'A Scheme for Estimating the Vertical Dispersion of a Plume from a Source near Ground-Level', Proceedings of the Third Meeting of the Expert Panel on Air Pollution Modelling, NATO Committee on the Challenges of Modern Society, Paris, France, October 1972.

Tennekes, H.: 1979, 'The Exponential Lagrangian Correlation Function and Turbulent Diffusion in the Inertial Subrange', *Atmos. Environ.* **13**, 1565–1567.

Thompson, R.: 1971, 'Numeric Calculation of Turbulent Diffusion', *Quart. J. Roy. Meteorol. Soc.* **97**, 93–98.

van Ulden, A. P.:1978, 'Simple Estimates for Vertical Diffusion from Sources near the Ground', *Atmos. Environ.* **12**, 2125–2129.

Vogt, K. J., Geiss, H., and Polster, G.: 1978, 'New Sets of Diffusion Parameters resulting from Tracer Experiments with 50 and 100 m Release Height', Proc. of Ninth Int. Tech. Meeting on Air Pollut. Modelling and its Applic., No. 103, NATO Committee on Challenges to Modern Society, 221–239.

Wamser, C. and Muller, H.: 1977, 'On the Spectral Scale of Wind Fluctuations within and above the Surface Layer', *Quart. J. Roy. Meteorol. Soc.* **103**, 721–730.

Wilson, J. D., Thurtell, G. W., and Kidd, G. E.: 1981a, 'Numerical Simulation of Particle Trajectories in Inhomogeneous Turbulence. I: Systems with Constant Turbulent Velocity Scale', *Boundary-Layer Meteorol.* **21**, 295–313.

Wilson, J. D., Thurtell, G. W., and Kidd, G. E.: 1981b, 'Numerical Simulation of Particle Trajectories in Inhomogeneous Turbulence. II: Systems with Variable Turbulent Velocity Scale', *Boundary-Layer Meteorol.* **21**, 423–442.

Wilson, J. D., Thurtell, G. W., and Kidd, G. E.: 1981c, 'Numerical Simulation of Particle Trajectories in Inhomogeneous Turbulence. III: Comparison of Predictions with Experimental Data for the Atmospheric Surface Layer', *Boundary-Layer Meteorol.* **21**, 443–464.

Yokoyama, O.: 1971, 'An Experimental Study of the Structure of Turbulence in the Lowest 500 Meters of the Atmosphere and Diffusion in it', Reports of the National Institute of Pollution and Resources (Japan), No. 2.